Thermo-elastostatic analyzes of new dampers made of polymer springs with negative thermal expansion

J Murín, V Goga, J Paulech, J Hrabovský, T Sedlár, V Kutiš, M Aminbaghai

Faculty of Electrical Engineering and Information Technology, Slovak University of Technology in Bratislava, Department of Applied Mechanics and Mechatronics of IAMT, Ilkovičova 3, 812 19 Bratislava, Slovakia
Vienna University of Technology, Vienna, Austria

justin.murin@stuba.sk

Abstract. The article presents original results of research of the dampers with passive and semi-active damping using polymer springs (also artificial muscles or nylon springs) with negative thermal expansion. Passive damping can be ensured by the strong damping effects of polymer springs. Semi-active damping can be provided by heating the springs from an additional heat source. According to design such dampers, mathematical models for analytical elastostatic and thermoelastostatic analyzes of dampers for selected load cases are processed in the paper. The permissible values of mechanical and thermal load of the dampers are determined. The obtained results are verified by numerical analysis using the finite element method. The elastostatics of the passive damper and its damping functionality have been verified on a real model of the damper. The compiled mathematical models can be used in the design of polymer dampers as well as in their automatic control. Designed and analysed dampers can be used in smaller mobile or stationary systems such as scooters, small car kits and the like. The elastodynamic functionality of the dampers with passive and semiactive damping will be presented and discussed in our further paper.

1. Introduction

The flexible suspension of mechanical elements and systems serves to eliminate the adverse effect of static and dynamic forces, thus achieving a higher quality of safe operation of the suspension system. The suspension also protects against damage and wear to the suspension systems. Typical examples are systems with passive, semi-active and active damping. Flexible support systems are used in both mobile and stationary systems. The passive suspension system is a conventional device that consists of a metal spring and a damper. With active suspension, the system parameters may change during operation. Active suspension can be controlled hydraulically, pneumatically or electromagnetically. Materials that have a high stiffness and strength are used for spring systems. In mechatronics, various types of artificial muscles have been used for a long time that mimic natural muscle and can change their stiffness, reversibly contract, expand or rotate within a single component due to an external stimulus (tension, current, pressure or temperature), electro active polymers (EAPs), supercoiled polymer (SCP), pneumatic artificial muscles (PAMs), or shape memory alloys (SMA). The efficiency of these systems is lower and requires higher energy inputs to control them. Polymers and nylon fibers, which are commonly used as a fishing line, can be effectively used as an integral part of the

mechatronic system, which is conditioned by the torsional load on the fiber, which causes its deformation and subsequent change in placement of fibrillar elements in the monofilament. In the literature, such a system is also called artificial muscle. From a practical point of view, this means that the polymer fiber must be twisted into a spring shape by means of a controlled twisting process. Immediately after winding the spring, the adjacent coils are in contact and represent a prestressed spring, which limits shrinkage during activation, and therefore the coils must be separated by increasing the longitudinal load. If adjacent coils are in contact, the thermal expansion of the muscle remains positive due to insufficient load or excessive twisting. If adjacent coils are not in contact due to additional tensile loading, the thermal expansion of the muscle is negative and the muscle performs mechanical work, as published in the most prestigious scientific journal "Science" in 2014 as a scientific discovery [1].

Recently, several researches around the world have been concerned with the characterization of such artificial muscles by experimental and computational methods, and their practical applications are being sought. In particular, it is a question of determining their mechanical and thermo-mechanical properties and practical applications of polymer springs. In the article [2] a new polymeric artificial muscle based on a composite was prepared and characterized. The work [3] presents an artificial muscle made of nylon fishing line, which is used to convert thermal energy into electrical energy. The results of experimental research of thermo-mechanical properties of nylon muscle are published in the article [4]. The work [5] deals with the current state of research of macroscopic artificial muscles, which work on the basis of electro-thermal excitation. The article [6] presents an artificial muscle made of twisted nylon 6.6 fiber. This article presents an effective phenomenological constitutive model, which contains several physical properties of artificial muscle. Paper [7] describes the mechanical behavior of nylon drives and investigates the elasticity and strength of the nylon spring as a function of temperature. The work [8] presents a new structure of biomimetic nylon drive, which mimics the human muscle with the ability to change stiffness and tensile strength by adding additional fibers. The work [9] presents technical data on the production process of selected artificial muscle drives. The construction of a new artificial muscle to drive an artificial robotic arm and the results of its experimental research are described in [10]. The work [11] describes an artificial muscle replacement made of ionometric composite. Multiscale approaches are also used to model these structures [12]. Comparison of modeling results and experimental results showed excellent agreement. In the work [13] a new type of support system simulating the movement of the human body driven by muscle contractions is proposed. The main characteristic of the above references is that experimental methods are used for the research of artificial muscles in conjunction with analytical calculations according to phenomenological relationships. In author's previous works [14-17], the results of our team on the area of research and application of the nylon springs are presented.

Prior art vibration dampers, due to their higher weight and dimensions, are less suitable for both passive and semi-active vibration damping with flexible properties for small mobile or stationary systems, such as electric scooters or small car kits, and similar systems.

The aim of this paper is the design, modeling and simulation of dampers using polymer springs with negative thermal expansion. Analytical mathematical models for their elastostatic and thermo-elastostatic analyzes will be compiled for the damper with passive and semi-active damping using the results of measuring the mechanical and thermomechanical properties of nylon springs. Limit values of mechanical and thermal load of dampers will be set to maintain their functionality. The obtained results will be verified using the Finite Element Method (FEM). The results of modeling and simulation could be used in the design of the physical model of the dampers, the function of which will be experimentally investigated, and the measured results will be compared with the results of analytical mathematical models. Mathematical models will be used for further research to automatically control and manage semi-active dampers in their practical application of suspension in small mobile or stationary systems. The elastodynamic functionality of the dampers with passive and semiactive damping that are built of nylon springs with negative thermal expansion will be studied and discussed in our further works.

2. Design and mathematical modeling of polymer dampers

Consider a damper body consisting of a housing 5 of cylindrical or other cross-section, a rod with a guide disc 1 and 2 resiliently mounted by means of prestressed polymer springs 6 and 8, limiting stops 7 and 9, and other parts of the damper according to Fig. 1. All springs have the same stiffness defined by the spring constant k_m and the negative temperature constant k_T (Fig. 1). There are n - springs on both sides of the disc [20].

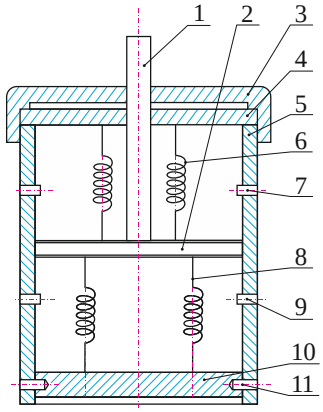

Figure 1. Physical model of a passive damper.

The initial length of each preloaded spring manufacturing process is l_0. The compressive prestressing force in one spring, which compresses the coils of the spring in contact with each other, is F_p. Said parameters are obtained by experimental measurements [14-17]. The neutral position of the damper represents the disk in the middle position, by which the clamped springs are mechanically extended to the length $l_m = l_0 + \frac{\Delta l_m}{2}$, where Δl_m is the elongation of all the springs system. As follows from the measurement, the temperature constant of one spring depends on its mechanical elongation, which is caused by the tensile force $F_m = F_p + \frac{k_m \Delta l_m}{2}$. Said system composed of n springs on each side of the disc can be physically replaced by a system of two springs connected at point B in series according to Fig. 2 with stiffnesses $k_{mn} = nk_m$ and with prestressing compressive force $F_{pn} = nF_p$. The system assembled in this way is loaded at point B with a dynamic force with static magnitude F_b. The damping of the damper can be passive, which is caused by the internal damping of the springs. Semi-active damping can be activated by heating the springs on one or both sides of the disc by a temperature difference ΔT due to negative temperature change in the length of the spring. The negative temperature constant of each spring, determined by measurement or calculation, is k_T. This temperature constant will depend on the elongation $\Delta l_m/2$, resp. from the force that will make this extension. The temperature constant can be measured or determined for a previously unknown extension by the procedure described in this article later. The aim of the elastostatic or thermoelastostatic analysis is to determine the new position of point B and the reaction forces at points A and C after application of the appropriate load. From the point of view of safe damper design, it is necessary to determine the maximum permissible value of the force magnitude F_{bmax} as well as the maximum permissible heating of one group or both groups of springs by the temperature difference ΔT_{max}.

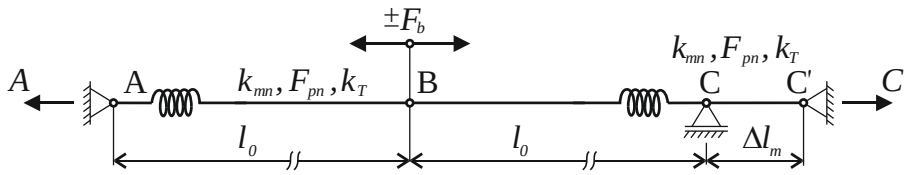

Figure 2. Equivalent damper model for *n* springs.

Mathematical models for analytical elastostatic, resp. thermo-elastostatic analysis of damper are assembled for a damper with passive as well as with semi-active damping. Passive damping uses the elastic and damping properties of the nylon springs, [22-23]. For semi-active damping, a change in the internal properties of the damper by heating the springs could be obtained. The results of the elastodynamic or thermo-elastodynamic analysis of the damper and dependence of the damping coefficient on the warming will be processed in our further research.

2.1. Elastostatic damper model with passive damping

The elastostatic model of the damper with passive damping for n = 1 is shown in Fig. 3. Its mathematical model consists of two loading steps, which are applied simultaneously to the equilibrium state. In the first step, a mechanical extension of the spring system by Δl_m is applied. In the second step, a force with magnitude F_b, which can act from the right to the left side or with the opposite orientation, starts to act at point B. Its maximum value is obtained from the elastostatic calculation. After application of the mechanical extension at point C according to Fig. 3, this point is shifted to position C′ by the value Δl_m, and point B is shifted to position B′ by the value $\Delta l_m/2$. Then the force required for this deformation for n springs on each side of the piston is $F_{mn} = F_{pn} + k_{mn}\Delta l_m/2$. For the supporting reactions at points A and C holds: $A_m = -C_m = F_{mn}$. The new length of the springs is $l_m = l_0 + \Delta l_m/2$.

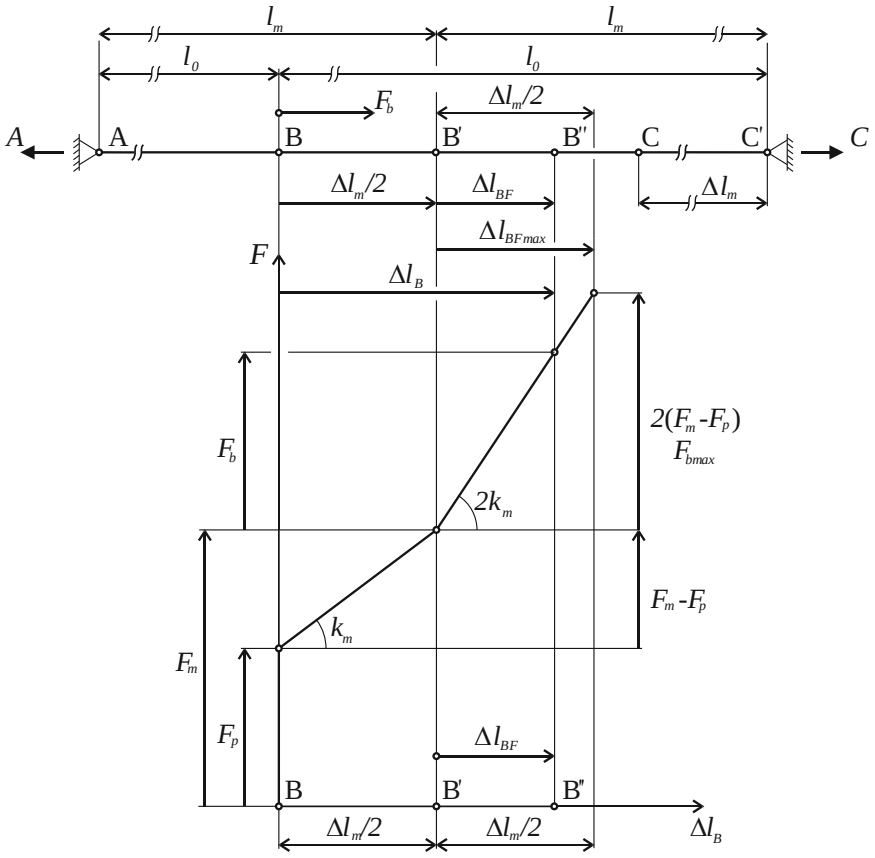

Figure 3. To the computational model of the elastostatic of the damper with passive damping for n = 1.

By applying a static force F_b to the point B′ according to Fig. 3, this is moved to the position B′′ by the value Δl_{BF}, and the reactions A_{mF} and C_{mF} occur in the supports. The reaction forces at points A and C′ can be determined by the II. Castigliano theorem: $C_{mF} = F_{mn} - F_b/2$ and $A_{mF} = F_{mn} + F_b/2$. Using I. Castigliano theorem, it is possible to determine the displacement of the point B′ to the point B′′ in the form $\Delta l_{BF} = \frac{F_b}{2k_{mn}}$. Then the displacement of point B to B′′ is $\Delta l_B = \frac{\Delta l_m}{2} + \Delta l_{BF}$. The new spring lengths are: $l_1 = l_m + \Delta l_{BF}$, and $l_2 = l_m - \Delta l_{BF}$. As can be seen from Fig. 3 and for n springs, the maximum permissible magnitude of the force F_b acting from left to right results from the condition $\Delta l_{BFmax} = F_{bmax}/2k_{mn} \leq \Delta l_m/2$. Then, $F_{bmax} \leq \frac{2k_{mn}\Delta l_m}{2} = 2(F_{mn} - F_{pn})$. Otherwise, the right already retracted springs would continue to compress to a length less than l_0, which is an unacceptable condition for the system. This condition determines the position of the limiting stops in the damper housing for the maximum deflections of the disc to one side or the other. The reciprocal situation occurs under the action of the oppositely oriented force F_b. As follows, the maximum amplitude of the force F_b can be increased by increasing the number of springs and their stiffness, as well as by increasing the initial elongation of the springs Δl_m.

2.2. Computational model of thermo-elastostatic of a damper with semi-active damping

Semi-active damping of the damper can be achieved by changing the internal tension of the system by heating all the springs on both sides or only on one side of the movable disk, which are mechanically stretched by a value of $\Delta l_m/2$ similar to that of a passive damper.

2.2.1. Thermo-elastostatic damper with heating of all springs

When all springs are heated, the mathematical thermo-elastostatic model of a spring damper with semi-active damping contains three steps that take into account the sequence of mechanical and thermal loading of the damper. It is the application of elongation of the spring system by Δl_m, warming of springs with temperature constant k_T by temperature difference ΔT, and loading at point B by a force with magnitude F_b, which can act from right to left, or reciprocally, from left to right. Following the procedure described in chapter 2.1, after extending the springs system at point C by Δl_m, we obtain the damper system in the state simply depicted in Fig. 4, which shows the state for n = 1. A similar diagram can be obtained for $n > 1$. If in this state all the springs are heated by the temperature difference ΔT, then due to the boundary conditions, this heating does not cause the point B´ to shift, because it is eliminated by the thermal force F_T that can be obtained from deformation condition $\frac{F_{T\varepsilon} 2 l_m}{nES} - 2\Delta l_T = 0$, where $\Delta l_T = k_T \Delta T$ is the intended thermal shortening of the springs on one side of the disc - see Fig. 4 (for n = 1). Then the temperature force $F_{T\varepsilon} = n\frac{ES}{l_m} k_T \Delta T = \varepsilon k_{mn} k_T \Delta T$, using the stiffness adjustment of the stretched springs $n\frac{ES}{l_m} = n\frac{ES}{l_0}\frac{l_0}{l_m} = \varepsilon k_{mn}$, where $\varepsilon = l_0/l_m$. There, *ES* is the effective tensional stiffness of the spring with the effective elasticity modulus *E* and the effective cross-sectional area *A*. The parameter ε takes into account the fact that we heat the length of the springs l_m and not l_0. As a result of warming, the reaction forces increase to the values: $C_{mFT} = C_{mF} + F_{T\varepsilon}$, $A_{mFT} = A_{mF} + F_{T\varepsilon}$. As shown in Fig. 4, for ε = 1 and n = 1, the temperature force is $F_T = k_m k_T \Delta T$. Since ε <1, the temperature force $F_{T\varepsilon} < F_T$. For smaller mechanical extensions, the parameter ε = 1 can be considered for simplicity.

The critical warming of all springs depends on the thermo-mechanical condition of the springs, in which the nylon fiber is glassed and thus the damper loses its functionality. As stated in the cited literature, this critical temperature depends of the nylon type and can be up to 150 ℃ and the thermal maximum contraction of the springs can be up to 49 – 65 %, [24].

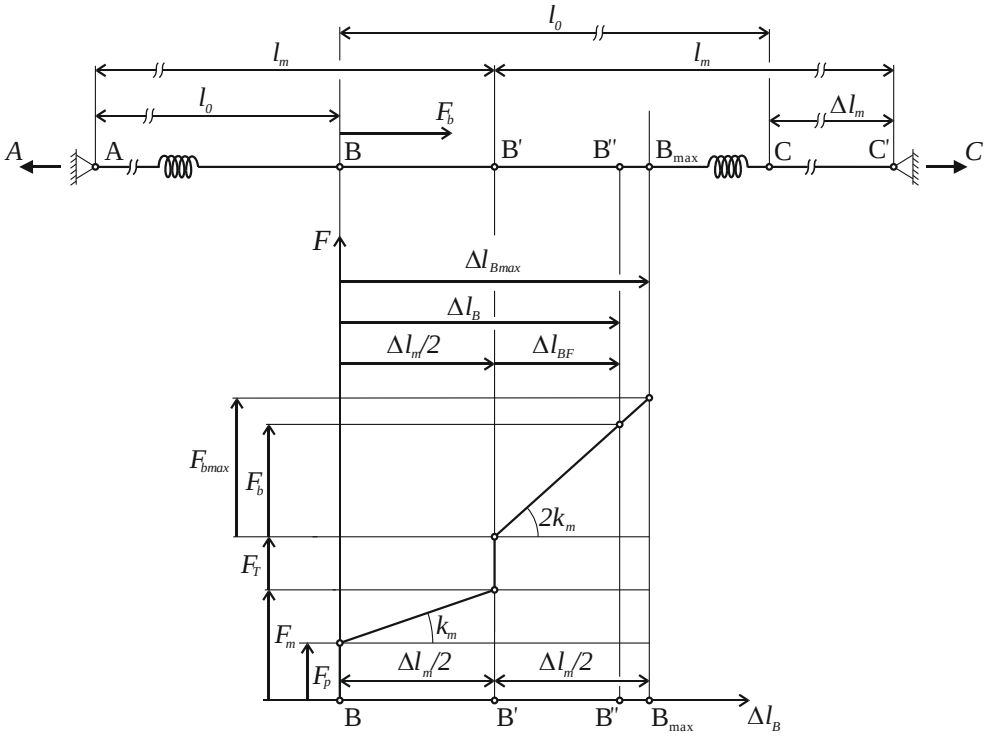

Figure 4. The dependence of displacement of point B on the applied load when heating the left and right springs for n = 1 and ε = 1.

By applying the force F_b to the point B′, it is shifted to the point B″ by the value $\Delta l_{BF} = \frac{F_b}{2k_{mn}}$. This relationship can be obtained using I. Castigliano's theorem. Then $l_1 = l_m + \Delta l_{BF}$, and $l_2 = l_m - \Delta l_{BF}$ are the final lengths of the springs. Further, $A = A_{mFT} + {F_b}/{2}$ and $C = C_{mFT} - {F_b}/{2}$ are coupling reactions. The total displacement of point B is $\Delta l_B = \frac{\Delta l_m}{2} + \Delta l_{BF}$. The maximum force magnitude F_b results from the condition: $\Delta l_{BFmax} \leq \frac{\Delta l_m}{2} = \frac{F_{bmax}}{2k_{mn}}$. Then $F_{bmax} \leq k_{mn}\Delta l_m = 2(F_{mn} - F_{pn})$. As can be seen from this result, the heating of all springs does not affect the magnitude of the allowable force F_{bmax} compared to its magnitude with a passive damper. However, this warming increases the tensile axial force in the springs, which affects the damping properties of the damper and increases their natural frequency. As is known, the tensile axial force increases the natural frequency of the bars and the compressive force reduces it, [21].

2.2.2. The damper with heating of one group of springs

Based on the above knowledge, from the point of view of further controlling the damper functionality and increasing the force magnitude F_b, in the considered case of its orientation it is suitable to thermally shorten e.g. only left springs of length l_m, because these can subsequently be extended by force F_b by a maximum value equal to elongation Δl_m - see Fig. 5 for n = 1. After heating the left n-springs by the value ΔT, the point B′ moves to the left to the point B″ by the value $\Delta l_{BT} = k_T \Delta T = F_T 2l_m/nES$. By introducing the ratio $\varepsilon = l_0/l_m$we get the required temperature force $F_T = \varepsilon k_{mn} k_T \Delta T/2$. For ε = 1, $F_{Tmax} = k_{mn}\Delta l_m/2$. The maximum warming of the left springs can reach the value $\Delta T_{max} = \Delta l_m/k_T$, while the maximum temperature shift of point B is $\Delta l_{BTmax} = \Delta l_m/2$, and the maximum temperature force $F_{Tmax} = \varepsilon k_{mn}\Delta l_m/2$. By applying the force F_b, the point B″ is moved to the point B‴ by the value $\Delta l_{BF} = F_b/2k_{mn}$. The maximum displacement of point B by force F_b is $\Delta l_{BFmax} \leq \Delta l_m = \frac{F_{bmax}}{2k_{mn}}$. Then the maximum force $F_{bmax} \leq 2k_{mn}\Delta l_m = 4(F_{mn} - F_{pn})$. It follows that the maximum amplitude of the force F_b can be up to twice that of the two previous dampers. The total displacement of point B to point B‴ is $\Delta l_B = \frac{\Delta l_m}{2} - \Delta l_{BT} + \Delta l_{BF}$. The resulting reactions forces are: $A = F_{mn} + F_T + F_b/2$, $C = F_{mn} + F_T - F_b/2$. The resulting spring lengths are: $l_1 = l_m - \Delta l_{BT} + \Delta l_{BF}$, and l_2=$2l_m - l_1$.

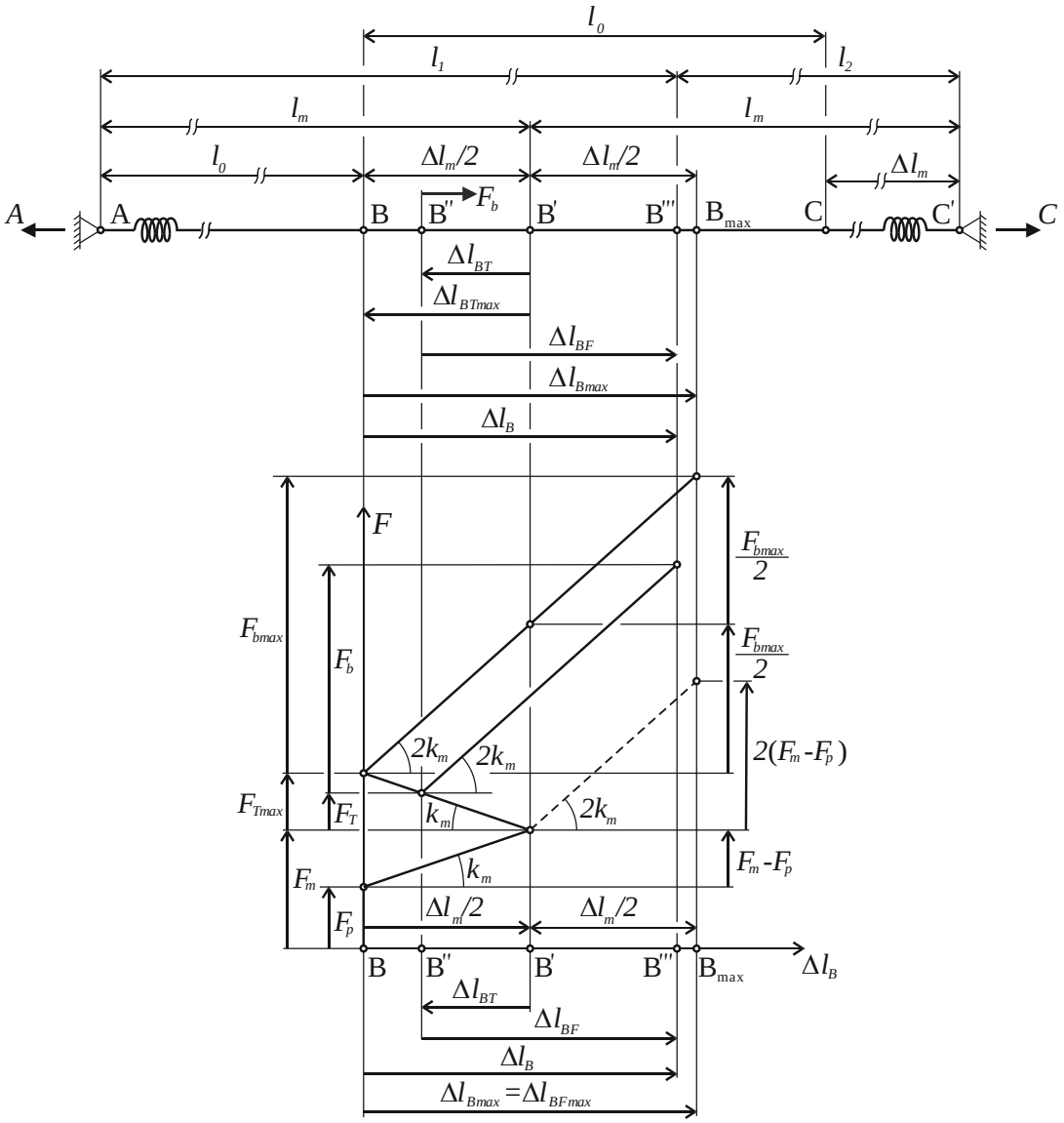

Figure 5. Dependence of the displacement of point B on the load of the damper for n =1 and ε = 1.

2.2.3. Experimental-computational determination of the temperature constant of a thermally shortened spring

As follows from the above damper models, the temperature constant of the respective spring k_T depends of the mechanical load and it must be measured. If no, it can be determined from the following experiments and computations. The selected vertically oriented spring attached at its upper end is loaded at its lower end with a mass m (Figs. 6 − 7) that represents the tensile force $F_m = mg$, where g is the gravitational acceleration. As mentioned above, this force elongates the spring with the spring constant $k_m = \tan\alpha_m$, compressive prestressing force F_p and with an initial length l_0, by known value Δl_m to the length l_m. The required force is $F_m = F_p + k_m\Delta l_m$. By heating the elongated spring by known temperature difference ΔT it is shortened by the measured value $\Delta l_T = k_T\Delta T$. The unknown temperature constant is $k_T = \Delta l_T/\Delta T$. It is obvious that the thermal constant of a relevant spring depends on its mechanical extension Δl_m, resp. on the magnitude of the force F_m that the thermomechanical internal force must overcome. In a system of several springs, the axial forces of the individual springs are mostly unknown, and therefore it was necessary to design the following

experimental-computational model for determining the unknown temperature constants. Assume the performance of two measurements of the shortening of an applied spring loaded by two different forces $F_{m1} > F_{m2}$, which are heated by the same temperature difference ΔT.

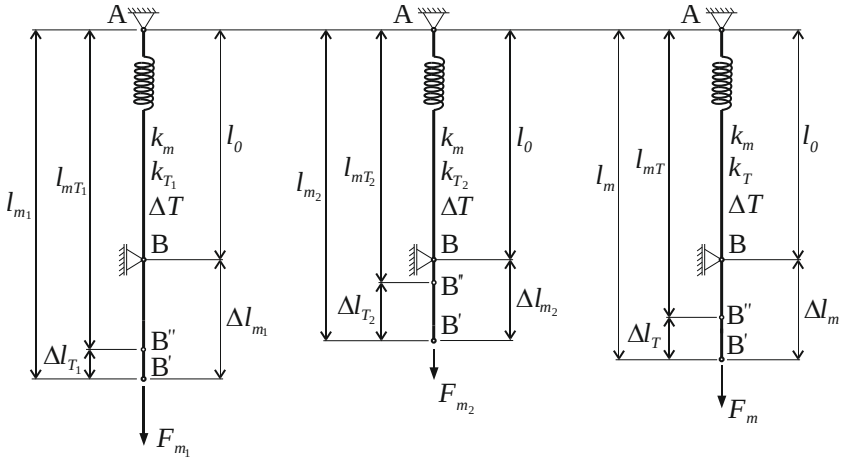

Figure 6. Measurement and calculation of the temperature constant of an applied spring.

According to Figs. 6−7, the applied spring is shortened by the values $\Delta l_{T_1} < \Delta l_{T_2}$, where $\Delta l_{T_1} = k_{T_1}\Delta T$ and $\Delta l_{T_2} = k_{T_2}\Delta T$. We assume a linear relationship between the loading forces and the temperature constants according the diagram in Fig. 7. From this dependence it is possible to determine new thermomechanical spring parameter λ, which applies to $F_m \in \langle F_{m2}, F_{m1}\rangle$:

$$\lambda = \tan\gamma = \frac{F_{m1}-F_{m2}}{k_{T2}-k_{T1}} = \frac{F_{m1}-F_m}{k_T-k_{T1}} = \frac{F_m-F_{m2}}{k_{T2}-k_T}\,. \tag{1}$$

Using this parameter, it is possible to determine the temperature constant for the selected elongation Δl_m, or the resulting force F_m

$$k_T = \frac{F_{m1}-F_m}{\lambda} + k_{T1} = \frac{F_m-F_{m2}}{\lambda} + k_{T2}\,. \tag{2}$$

If the temperature constant was measured for F_m equal to F_{m1} resp. F_{m2}, then k_T is equal to k_{T_1} resp. k_{T_2}. For our dampers $F_m = F_p + k_m\Delta l_m/2$.

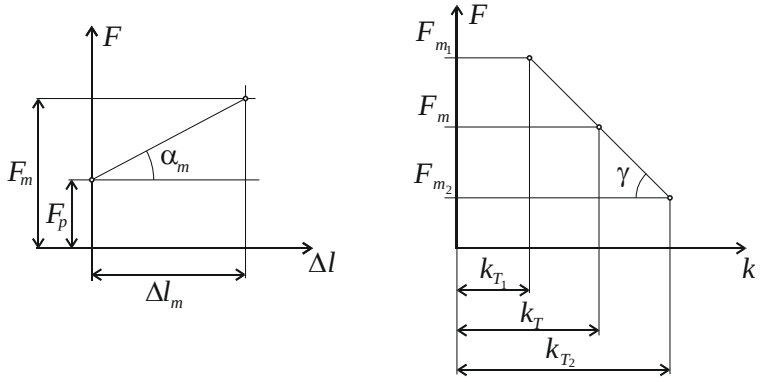

Figure 7. Measurement and calculation of the spring and thermal constants.

The temperature constant k_T thus obtained for unmeasured mechanical elongation Δl_m is independent on a value of the applied heating ΔT. To determine more accurately the thermomechanical parameter of the spring, measurements can be made in more load cases than two, and this parameter λ can be determined as the mean value of these measurements, thus eliminating their possible nonlinearity. As

the measurement results showed, this dependence can be considered as linear. It should be noted that negative temperature constants are reported here in their absolute value.

3. Computational experiments

Based on the compiled mathematical models, semi-analytical analyzes of all three types of dampers were performed. The following subchapters present the results of analytical calculations for individual dampers. The obtained results are verified by the finite element method (FEM), [19]. As the measurement showed, the nylon spring behaves almost linear even with its large elongation and shortening. One link finite element for one spring with artificial axial spring stiffnesses $ES/l_0 = k_m$ was used to model the springs. At the initial length of the spring l_0, it is possible to determine the cross-sectional stiffness with the effective modulus of elasticity E and the artificial cross-sectional area S from the measured spring constant. Then the compressive prestressing stress of the beam is $\sigma_p = F_p/S$. In the passive model, the beam is fixed at point A with a fixed joint and at point B with a sliding joint in the direction of the x-axis. At point C, where the sliding joint is in the direction of the x-axis, the mechanical elongation Δl_m is prescribed, and at point B the loading force F_b is aplied. Using linear analysis, the displacement of point B and the reaction forces at points A and C can be determined. In addition to the passive damper, the coefficient of thermal contraction α_T must be determined for the thermal load of the replacement link. We get this from the known temperature constant k_T from the condition: $\alpha_T l_m \Delta T = k_T \Delta T$. Foreign, $\alpha_T = k_T / l_m$. Since in fact the length of the extended spring l_m is heated, then $\alpha_T \frac{k_T}{l_m} = k_T/(l_0 + \Delta l_m/2)$. However, if the loading took place simultaneously with the displacement of the point C, the loading with the force F_b and the heating of the ΔT , then it would be possible to consider l_0 as the warmed length of the beam. Then $\alpha_T = k_T/l_0$. Both options were used by the FEM solution to compare the results, and the same differences in the results were found as in relevant tables for the case $\varepsilon = 1$, resp. $\varepsilon = l_0/l_m$. As already mentioned, the agreement of the results by analytical models and numerical models with FEM has been excellent.

3.1. Elastostatic analysis of a passive damper

Tab. 1 shows the initial parameters of the springs and their permissible maximum load, as well as the number of springs n on each side of the disc. Tab. 2 shows the results of the analytical solution for different values of elongation Δl_m, spring constant k_m, prestressing force F_p, force F_b as well as for $n = 1$ and $n = 4$ springs in series-parallel arrangement.

Table 1. Initial and permissible maximum parameters of the passive damper.

i case	l_0 [mm]	Δl_m [mm]	k_m [N/mm]	F_p [N]	F_{bmax} [N]	Δl_{BFmax} [mm]	n
1	105	5.36	0.212	2.1	1.136	2.68	1
2	105	9.99	0.212	2.1	2.12	4.99	1
3	105	14.62	0.212	2.1	3.10	7.31	1
4	80	20.00	0.260	1.0	5.20	10.00	1
5, 6	80	20.00	0.260	1.0	20.80	10.00	4

As can be seen from Tab. 1, the maximum allowable force amplitude F_{bmax} increases with increasing elongation Δl_m and with increasing stiffness k_m. As the number of springs n increases, this force increases n – times logically. The maximum displacement of the point B caused by the force F_b is limited by one half of the elongation Δl_m.

Table 2. Solution results by analytical method for the passive damper.

i case	F_m [N]	F_b [N]	Δl_{BF} [mm]	Δl_B [mm]	A [N]	C [N]	l_m [mm]	l_1 [mm]	l_2 [mm]	n
1	2.67	1.13	2.67	5.34	3.23	2.10	107.68	110.34	105.01	1
2	3.16	1.13	2.67	7.66	3.72	2.59	109.99	112.66	107.33	1
3	3.65	1.13	2.67	9.98	4.21	3.08	112.31	114.97	109.64	1
4	3.60	1.13	2.17	12.17	4.16	3.03	90.00	92.17	87.82	1
5	14.40	1.13	0.54	10.54	14.96	13.83	90.00	90.54	89.46	4
6	14.40	9.81	4.71	14.71	19.30	9.49	90.00	94.72	85.28	4

From the point of view of safe operation, the initial extension of the spring is limited by the state in which, as a result of this load, the springs begin to unwind and destroy. This elongation value must be determined by measurement. From the analyzes results given in Tabs. 1-2 also follows that with a large number of these cheap and light springs with a higher spring constant, the passive damper can transmit relatively large forces and can therefore be used for flexible suspension of smaller mobile or stationary systems. The damping of the passive damper itself is given by the mechanical properties of polymer springs, the experimental results of which will be presented in our next article. The results shown in Tab. 1 and 2 were verified by calculation by the finite element method by a linear model, which is described in more detail in the introduction to Chapter 3. Excellent agreement of all results was achieved. Therefore, in order to shorten the scope of the tables, these values are not repeated in those tables.

To assess the results of the elastostatic simulation, the passive damper was manufactured, assembled with the parameters listed in the last line of Tab. 1. For the load parameters listed in last line (case i = 6) in Tab. 2, the displacement of the point B with a force $F_b = 9.81$ N of magnitude $\Delta l_{BF} = 4.1$ mm was found by measuring the produced damper. The acceptable difference to analytical solution of 4.71 mm is caused by uncertainty of the measurement.

To show the excellent passive damping effects of the nylon springs, the free vibration test - measurement of the reaction force on the damper's support was performed. The prototype of the damper with n = 4 nylon springs is shown in Fig. 8. The damper body consists of a plexiglass tube in which fixed handles for nylon springs are attached at the ends. In the middle of the damper there is a movable piston on which the free ends of the springs are attached. The handles are held so that the springs are stretched to the required length l_m – see Tab. 1, the case 5, 6. Both the handles and the piston were made of PLA material using 3D printing. The piston rod is attached to the piston and is subjected to an external load.

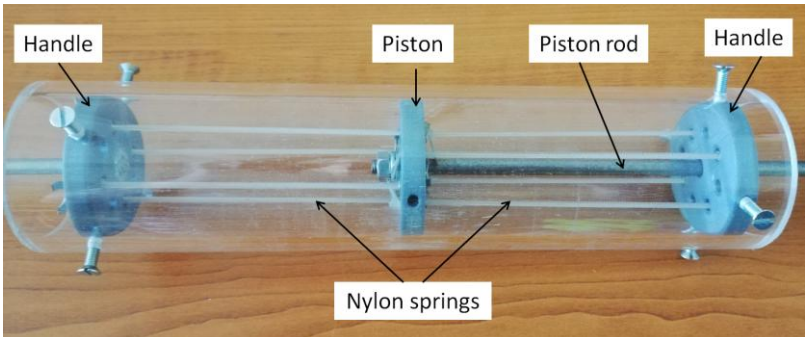

Figure 8. Prototype of the passive damper with n = 4 nylon springs.

The damping effect of the damper is presented in Fig. 9, where the time course of the measured reaction force on the damper's support is shown. During the test, the damper was loaded by free vibration of the loading mass equal to 1 kg, Fig. 10.

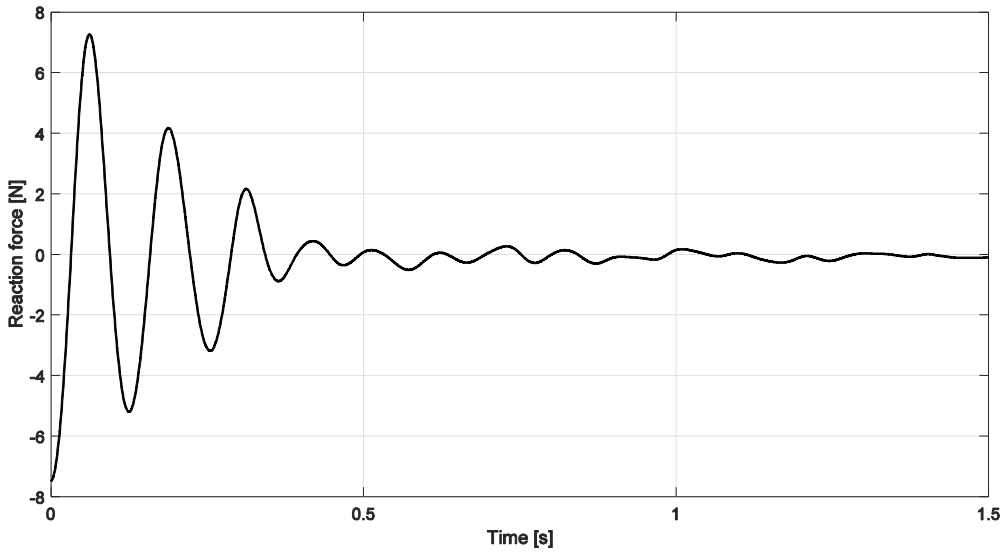

Figure 9. The time course of the measured reaction force on the damper's support.

Figure 10. Free vibration test - measurement of the reaction force on the damper's support.

As shown in Fig. 9, the free oscillation of the applied mass was attenuated very fast in 1.5 seconds.

3.2. Thermo-elastostatic analysis of a semi-active damper with heating of all springs

Based on the compiled mathematical model given in chapter 2.2.1, a thermo-elastostatic analysis of the semi-active damper for n = 1 springs on both sides of the disc was performed. In all cases $i = 1-3$ from Tab. 3, the same springs were used with the following parameters, which were obtained by measurement: the spring constant $k_m = 0.212$ N/mm, the compressive prestressing force $F_p = 2.1$ N and the initial length of the spring $l_0 = 105$ mm. According to Fig. 4, by mechanical displacement Δl_{mi}, the point B of one measured spring has shifted to the point B′.

The force F_{mi}=F_p +$k_m \Delta l_{mi}$ corresponds to this displacement of point B of one spring. The measurement of the temperature constant k_{Ti} of this spring was performed for three values of displacement Δl_{mi} of point B to point B′, which correspond to the respective values of forces F_{mi}= $m_i g$, (Fig. 7 −8), where $g = 9.81$ ms^2 is gravitational acceleration. In a system of two springs

connected in series, point *B* is shifted by the value $\Delta l_{mi}/2$, so that the corresponding tensile force in the spring is F_m. The results of the measurement of the temperature constant k_{Ti} of the applied spring are given in Tab. 3. The applied spring, loaded with three different weights, was heated by $\Delta_T = 10$℃ in each measurement.

Table 3. Initial parameters of the semi-active dampers.

i case	m_i [kg]	F_{mi} [N]	F_m [N]	Δl_{mi} [mm]	k_{Ti} [mm/℃]	Δl_{Ti} [mm]	k_T [mm/℃]	ε [-]
1	0.33	3.24	2.67	5.36	0.322	3.22	0.327	0.975
2	0.43	4.22	3.16	9.99	0.311	3.11	0.322	0.954
3	0.53	5.20	3.65	14.62	0.302	3.02	0.317	0.935

The mean value of parameter (1) is λ = 98.82 N ℃ / mm. The temperature constants k_{Ti} of one applied spring in the dampers for the respective displacements Δl_{mi} of point C to point C′, resp. corresponding tensile forces F_{mi} are given in Tab. 3. The unknown temperature constants k_T for the spring in the damper loaded by the forces F_m, is calculated according to equation (2) and is given in the Tab. 3. These temperature constants enter into the thermo-elastostatic analysis of semi-active dampers with heating of all springs as well as only springs on one side of the piston. The applied extensions Δl_{mi} are also listed in Tab. 3. Both springs are warmed by a temperature difference ΔT = 10 ℃. At point B, the force F_b=1N is applied. The magnitude of the force F_{bmax} is the same as it is shown for the cases 1-3 in Tab.1. The maximum warming temperature, ΔT_{max}, is constraint by the glass transition temperature of the nylon 6.6.

3.3. Thermo-elastostatic analysis of a semi-active damper with heating of one group of springs

As follows from chapter 2.2.2, the procedure of analysis of this damper differs from the previous case only in the calculation of the thermal force, which is induced by the thermal shortening, e.g. of the left spring - see Fig. 6. The heating of one spring, resp. of one group with *n* springs, causes the displacement of the point B, thus creating space for increasing the magnitude of the force F_{bmax}. The input parameters of the analysis are the same as given in Tab. 3. The left spring is warmed by ΔT = 10 ℃. At point B, the force F_b=1N acts. The results of the analysis are given in Tab. 4 for the parameter ε = 1 and *n* = 1. For *n* > 1, the displacement of point B from the force F_b decreases proportionally.

Table 4. Results of semi - active damper analysis for parameter ε = 1 and *n* = 1.

i	Δl_{mi} [mm]	F_m [N]	Δl_{BT} [mm]	Δl_{BF} [mm]	Δl_B [mm]	l_m [mm]	l_1 [mm]	l_2 [mm]	A [N]	C [N]
1	5.36	2.67	1.64	2.36	3.40	107.68	108.40	106.96	3.51	2.51
2	9.99	3.16	1.61	2.36	5.74	109.99	112.35	107.64	4.00	3.00
3	14.62	3.65	1.59	2.36	8.08	112.31	113.08	111.54	4.48	3.48

In Tab. 5, a comparison of the essential results of the analyzes with the parameters ε = 1 and $\varepsilon = l_0/l_m$ is shown. The values of the parameter ε are given in the last column in Tab. 3. The results of the solution with the application of this parameter $\varepsilon = l_0/l_m$ are denoted by the index ε in Tab. 5.

Table 5. Comparison of results for *n* = 1 with ε = 1 and $\varepsilon = l_0/l_m$.

i	Δl_B	$\Delta l_{B\varepsilon}$	A	A_ε	C	C_ε
1	3.40	3.46	3.51	3.50	2.51	2.50
2	5.74	5.85	4.00	3.98	3.00	2.98
3	8.08	8.24	4.48	4.46	3.48	3.46

From the above comparison in Tab. 5, it is clear that taking into account the fact that the heating shortens the left spring by length l_m and not l_0 does not significantly affect the results of the analyzes. As the results of spring measurements show, their linearity is maintained even at higher values of elongation. The above results were verified by the above-mentioned linear FEM model [19]. As with the previous models, an excellent agreement of the results obtained by the finite element method [19] has been achieved in this case as well.

Table 6. To determine the maximum allowable warming ΔT_{max} and the maximum force F_{bmax} for $n = 1$.

i case	Δl_{mi} [mm]	ΔT_{max} [°C]	Δl_{BTmax} [mm]	Δl_{Bmax} [mm]	F_{bmax} [N]	F_{Tmax} [N]
1	5.36	16.36	2.68	5.36	2.27	0.57
2	9.99	30.96	4.99	9.99	4.23	1.06
3	14.62	46.02	7.31	14.62	6.20	1.55

As seen in Tab. 6, the force F_{bmax} is twice for as in the case of a passive damper and a semi-active damper with heating of both springs. Tab. 6 shows the limit values of the left spring heating Δ_{Tmax} and the force F_{bmax}. Increasing the number of springs n increases the maximum allowable force F_{bmax} n-times. The maximum heating of the springs as well as the total displacement of point B is limited by the displacement of point C. However, this displacement is limited by the mechanical destruction of the spring caused by the unwinding of its coils.

4. Conclusions

The content of the article is focused on the design and research of vibration dampers composed of prestressed polymer springs with negative thermal expansion. The springs were made by twisting nylon fibers 6.6, also known as "fishing line". Mathematical models of three types of dampers were established for their elastostatic, resp. thermo-elastostatic analysis by analytical method.

Passive damper elastostatic analyzes were performed, using the elastic properties of nylon springs. These properties were obtained by author´s measurement. The results of the analytical calculations were focused on the elastostatic deformation of the springs after their mechanical elongation and subsequent loading with chosen amplitude of the dynamic force, the static effects of which should be transmitted by the damper. Maximum values of the amplitude of the loading force were determined, the magnitude of which depends on the number of springs connected in series and parallel, on their stiffness, as well as on their mechanical extension to their operating state. These results were also verified by measurements on a real model of the damper, which was established for this purpose [20]. These measured results confirmed the correctness of the compiled mathematical model of the passive damper. To show the excellent passive damping effects of the nylon springs, the free vibration test - measurement of the reaction force on the damper's support was performed. As shown in Fig. 9, the free oscillation of the applied mass was attenuated in 1.5 seconds.

Thermo-elastostatic analyzes of the semi-active damper were performed for two cases of heating of its springs. For the case of heating of all springs, the thermo-elastostatic state of the springs caused by their mechanical elongation, thermal heating as well as loading by the selected static force was calculated. The permissible maximum values of the loading force were determined, the magnitude of which depended on the number of applied springs as well as on the mechanical elongation of the springs to their operating state. The maximum value of warming is limited by the temperature that causes the vitreous of the originally flexible polymer fiber to glaze, and for various types of nylon has been published in the article [1] and in the works cited therein. With the same initial extension of the springs as with the passive damper as with warming all of the springs, the maximum permissible value of the amplitude of this force is the same. However, the heating of all the springs significantly increases the tensile internal force in the springs, so that a change in the dynamic properties of the

damper can be expected. As is known, a large axial force significantly influences the stiffness of the bars, which then affects the dynamic properties. This impact will be explored in our further work.
For the case of heating one group of springs, thermo-elastostatic analyzes of the semi-active damper were performed. The results of the calculation showed that by heating one group, the value of the maximum value of the dynamic force can be doubled compared to the previous two types of dampers. A maximum value of spring warming was also determined, which is limited by the value of the initial mechanical elongation of the springs.
The results of all analytical calculations were verified by the finite element method using ANSYS software [19], while identical results of deformation as well as internal forces and reaction forces of the dampers were obtained. Therefore, the results of the solution with a truss finite element are not given in the tables containing the results of the analytical solution of the thermoelastic analysis of the investigated dampers.

The main benefit of the article is the modelling and design of a new type of dampers that can transmit relatively high values of dynamic force amplitude. An experimental calculation procedure for determining the temperature constant of applied springs was developed. The value of this constant depends on the magnitude of the axial force induced by the initial mechanical elongation of the applied springs. The established mathematical models can be used to design such dampers in the praxis, which are characterized by low weight and low cost. As the results of our partial research show, these dampers are also characterized by very good damping effects, which will also be possible to control by heating the springs, thus achieving their negative thermal expansion. These new types of dampers will be applicable to flexible support of small stationary and mobile systems. However, by using nylon springs with a high spring constant and a larger number of them, it will be possible to damp the effects of greater dynamic forces. The weakness of the application of nylon springs is their relatively high sensitivity to temperature changes, so that their more accurate applications will require their stabilization to the ambient temperature in which the system is operated. The elastodynamic functionality of the dampers with passive and semiactive damping that are built of nylon springs with negative thermal expansion will be presented and discussed in our further paper in more detail.

Acknowledgement: The authors gratefully acknowledge financial support by the Research and Development Agency under Contract No. APVV-19-0406.

References

[1] Haines CS et. al 2014 Artificial Muscles from Fishing Line and Sewing Thread *Science* **343** pp. 868-872
[2] Zhang P and Li G 2015 Healing-on-demand composites based on polymer artificial muscle *Polymer* **64** pp. 29-38
[3] Kim SH et al 2015 Harvesting temperature fluctuations as electrical energy using torsional and tensile polymer muscles *Energy and Environment Science* **15**
[4] Cherubini A, Moretti G, Vertechy R and Fontana M 2015 Experimental characterization of thermally-activated artificial muscles based on coiled nylon fishing lines *AIP Advances* **5**
[5] Otero TF and Martinez JG 2015 Physical and chemical awareness from sensing polymeric artificial muscles *Experiments and modeling Progress in Polymer Science* **44**
[6] Sharafi S and Li G A multiscale approach for modeling actuation response of polymeric artificial muscles *Soft Matter* **19**
[7] Kianzad S et al 2015 Nylon coil actuator operating temperature range and stiffness *Electroactive Polymer Actuators and Devices 2015 Proc. SPIE 9430* ed. Y. Bar-Cohen (Bellingham WA: SPIE)
[8] Kianzad S et al 2015 Variable stiffness structure using nylon actuators arranged in a pennate muscle configuration *Electroactive Polymer Actuators and Devices 2015 Proc. SPIE 9430* ed. Y. Bar-Cohen (Bellingham WA: SPIE)
[9] Moretti G, Cherubini A, Vertechy R and Fontana M 2015 Experimental characterization of a

new class of polymeric-wire coiled transducers *Behaviour and Mechanics of Multifunctional Materials and Composites 2015 Proc. SPIE 9432*, ed. NC. Goulbourne (Bellingham WA: SPIE)
[10] Wu L et al 2015 Nylon-muscle-actuated robotic finger *Active and Passive Smart Structures and Integrated Systems* 2015 *Proc. SPIE 9431* ed. Wei-Hsin Liao (Bellingham, WA: SPIE)
[11] Zhang P et al 2016 Healing of polymeric artificial muscle reinforced ionomer composite by resistive heating *Journal of Applied Polymer Science* **133**
[12] Yang Q and Li G 2016 A top-down multi-scale modeling for actuation response of polymeric artificial muscles *Journal of the Mechanics and Physics of Solids* **92**
[13] Chen CY et al 2016 Motion Guidance Sleeve: Guiding the Forearm Rotation through External Artificial Muscles *CHI'16 Proc. of the 2016 CHI Conference on Human Factors in Computing Systems* 2016 (NY United States: Association for Computing Machinery) pp. 3272–76
[14] Murín J, Goga V, Hrabovský J, Búc D and Podešva P 2017 Measurement and numerical analysis of the artificial muscles made of fishing line *Advanced Materials Letters* **8** pp 635-640
[15] Minár M, Goga V, Čapková R, Ondrejička K and Murín J 2020 Basic parameters of coiled fishing line actuator *K&I 2020 Proc. of the 30th Int. Conf. on Cybernetics and Informatics*, ed. J. Cigánek et al. (New Jersey: Piscataway) pp. 204-208
[16] Murín J, Goga V, Hrabovský J, Podešva P and Gogola R 2016 Numerical analysis of the artificial muscle made of fishing line *APCOM 2016 Proc. of 22nd int. conf. on applied physics of condensed matter*, ed. J. Vajda and I. Jamnický (Slovakia: STU v Bratislave) pp. 231-235
[17] Minár M, Goga V and Murín J 2020 The main features of coiled fishing line actuator *ELITECH'20* (electronic source) *22nd Conf. of doctoral students* (Bratislava Slovakia: Spektrum STU)
[18] Wolfram MATHEMATICA 9.0.1.0. Wolfram Research, 2013.
[19] ANSYS Swanson Analysis System, Inc., 201 Johnson Road, Houston, PA15342/1300, USA.
[20] Murín J, Goga V and Sedlár T 2021 Vibration damper with coiled tension springs made of nylon Submission of a Utility model application (PUV 50026-2021) Slovak University of Technology in Bratislava, Slovakia.
[21] Aminbaghai M, Murín J and Kutiš V 2012 Modal Analysis of the FGM-Beams with Continuous Transversal Symmetric and Longitudinal Variation of Material Properties with Effect of Large Axial Force *Engineering Structures* **34** pp. 314-329
[22] Goga V, Hrabovský J, Šarkán L, Malinarovičová T and Paulech J 2018 Modelling and measurement of dynamic parameters of the nylon actuators *APCOM 2018: 24th Int. conf. on applied physics of condensed matter* Štrbské Pleso Slovak Republic June 20-22. 1. ed. St. Louis (AIP Publishing Art. no. 020031)
[23] Goga V, Minár M, Murín J, Kutiš V, Paulech J and Gálik G 2019 Basic parameters of coiled fishing line actuator *Applied mechanics 2019: 21st Int. conf.* Ostravice Czech Republic April 17-19 2019 (Ostrava: VŠB - Technická univerzita Ostrava) pp. 65-69
[24] Nurul Anis Atikah et al 2017 Development of nylon-based artificial muscles for the usage in robotic prosthetic limb *Advances in electrical and electronic engineering: from theory to aplications: Proc. of the Int. Conf. on Electrical and Electronic Engineering AIP conf. proc. 1883* ed. L Audah et al (Melville, NY: AIP Publishing)